Mechanistic Model Simulations of the East African Climate Using NCAR Regional Climate Model: Influence of Large-Scale Orography on the Turkana Low-Level Jet

MATAYO INDEJE, FREDRICK H. M. SEMAZZI, AND LIAN XIE

Department of Marine, Earth and Atmospheric Sciences, North Carolina State University, Raleigh, North Carolina

LABAN J. OGALLO

Department of Meteorology, University of Nairobi, Nairobi, Kenya

(Manuscript received 20 March 2000, in final form 20 September 2000)

ABSTRACT

The National Center for Atmospheric Research regional climate model (RegCM) is employed to study the dynamics of the Turkana low-level jet that lies between the Ethiopian and the East African highlands, and also investigate the mechanisms responsible for the observed dry conditions over the Lake Turkana basin that lies in the wider section of the Turkana channel. The role of the large-scale orography and two other forcing factors namely the large-scale monsoonal flow and the Turkana channel depth are investigated in order to understand the kinematics of the jet.

The simulated patterns of the Turkana easterly low-level jet compares well with its observed characteristics. Strong winds are indicated in the channel throughout the study period of October to December, with the wind speed decreasing in the middle and wider region of the channel. A split in the jet core is also shown in the middle of the channel. The level of maximum winds ($\sim$11 m s^{-1}) occurs in the layers 930-hPa and 650-hPa levels. The dynamics of the Turkana channel is explained in terms of the orographic channeling effects associated with the Bernoulli theorem as applied to barotropic steady and nonviscous flows. The main results on the forcing mechanisms responsible for the development of the jet can be summarized as follows: (a) orographic forcing is the most important factor, (b) the large-scale monsoon background flow is important in determining the wind speed in the jet cores, (c) the depth of the channel determines the vertical structure and location of the jet cores, and (d) thermal and frictional forcing play equivalent role as that of the large-scale background winds in the formation and maintenance of the jet. Divergence and anticyclonic vorticity partly explains the observed split in the jet cores in the middle of the channel. The dry conditions observed over the Lake Turkana basin are explained in terms of dominant downward vertical velocity, decrease in moisture flux convergence, and increase in temperature flux divergence that inhibit active developments of mesoscale circulations and their interactions with large-scale flow over these areas. The identified regions of strong winds associated with the jet are important to the safety in the aviation industry. These regions may also provide alternative renewable energy resources in the form of wind energy.

1. Introduction

The term orography implies obstacles on the large-scale such as mountain ranges, which affect stratified flows in the atmosphere. It is one of the lower boundary factors controlling global climate dynamics. Orography may influence climate through 1) its role in determining the positions of the semipermanent upper tropospheric troughs and ridges in the westerlies, 2) the orographic convective precipitation systems, 3) the role it plays in the development and maintenance of mesoscale circulations, and 4) the blocking and channeling effects on the low-level jetstreams. Whereas, the land/sea thermal contrast affects climate through thermal forcing, the effect of large-scale orography is mainly dynamical in nature (Kasahara 1966). Ringler and Cook (1999) have, however, recently shown that thermal forcing associated with topography is equally important in forcing atmospheric structure especially in the Tropics. The main effect of orography on the mean flow is through form drag that is associated with differences in tangential pressure across a mountain. In the globally averaged atmosphere, this is approximately 50% of the total drag from the ground, the other half being frictional drag associated with the turbulent boundary layer (Stull 1988). Regional climate may be influenced by the structure of the large-scale flow for that region and the presence or absence of other forcings such as orography, and mean heat sources and sinks. This is mainly the case in the Tropics where the dynamical flow instabil-

Corresponding author address: Fredrick H. M. Semazzi, Dept. of Marine, Earth and Atmospheric Sciences, North Carolina State University, Raleigh, NC 27607-8208.
E-mail: fred_semazzi@ncsu.edu

ities are relatively weak as compared to those in the midlatitudes (Xue and Shukla 1998).

Orographic forcing on regional weather and climate has been the subject of several major investigations ever since the pioneering work by Kasahara (1966). Sarker et al. (1978) showed that rainfall distribution over the Ghat mountains of India was dependent on orography and the latent heating that induces upward motion in both the heating area and downstream of the mountain. Semazzi (1980, 1985) investigated the influence of large-scale orographic forcing on the African climate using a primitive equation barotropic model, and showed an equatorial geopotential height trough and a pair of tropical anticyclones on either side of the equatorial trough. He indicated that the observed semi-permanent trough (Equatorial trough) in the middle troposphere over equatorial Africa is maintained partly by orographic forcing. Semazzi and Sun (1997) suggested that orographic control could play a critical role in maintaining the observed teleconnections between global SST anomalies and the West African droughts.

Unlike for West African midtropospheric jet, which is fundamentally related to the surface temperature and soil moisture distribution at the surface (Cook 1999) and perhaps modified by topography, the low-level jet streams over eastern Africa are forced mainly by the local orography (Krishnamurti et al. 1976; Anderson 1976; Ngara and Asnani 1978; Bannon 1979, among others). A low-level jet is typically a thin stream of fast-moving air with maximum wind speeds of 10–20 m s^{-1} that is usually observed in the lowest 1–2 km of the atmosphere. It is classified in the meso-β scale circulation with horizontal scales between 20 and 200 km, and timescales from hours to several days. Studies have shown that low-level jetstreams through the associated convergence/divergence and vertical motion patterns exert a control on the surface weather and climate (Hastenrath 1985). Low-level jets are also significant in the transport of pollution and pests, are potential sources of wind energy, may cause aircraft accidents due to the strong wind shears associated with them, and may also cause a sudden intensification and rapid spread of forest fires and sand storms.

Several studies have been carried out to investigate the influence of orography on regional climates (Sarker et al. 1978; Semazzi 1980, 1985; Semazzi and Sun 1997). These studies have indicated the importance of orography in shaping regional climates. The purpose of the present study is to investigate the role of orographic forcing in modulating the East African climate. A series of basic sensitivity studies are performed using a regional climate model (RegCM) to 1) investigate the dynamics underlying the orographic influence and other forcing mechanisms (the large-scale monsoon flow and the depth of the channel) on the Turkana low-level jet, and 2) understand the mechanisms responsible for the flow over the Turkana channel and specifically the observed desert conditions over parts over the valley. This

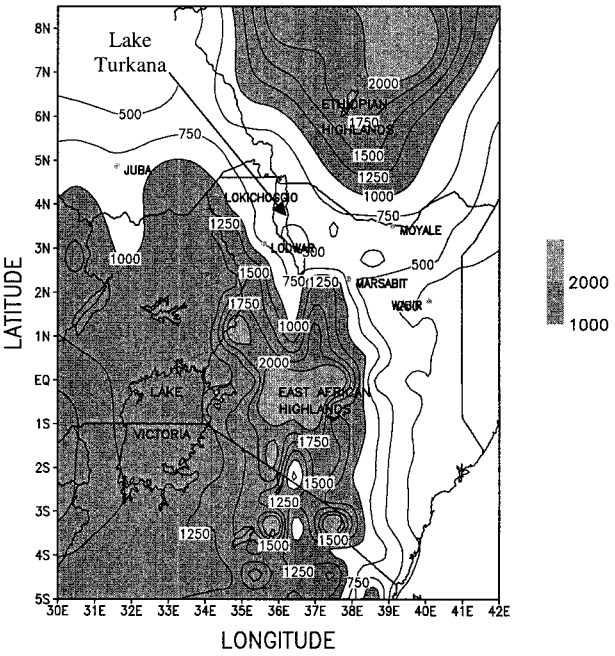

FIG. 1. Topography over the Turkana Channel. Terrain height values greater than 1000 m are shaded.

investigation is aimed at contributing to our basic understanding of the processes involved in establishing a time-mean climate over eastern Africa during boreal autumn season. Such an understanding is necessary in order to improve our ability to understand and predict the climate variability in the region.

Observational studies

East African region is enclosed by latitudes 9°N–10°S and longitudes 28°–42°E. It has diverse topographic features that include the Ethiopian highlands to the northeast and East African highlands to the southwest (Fig. 1). Some of the high mountain peaks in the region are Mount Kenya (5199 m), Mount Kilimanjaro (5895 m), Mount Elgon (4321 m), Aberdare Ranges (3999 m), and the Mau escarpment (3098 m). In between the Ethiopian highlands and the East African highlands lies the Turkana channel (Kinuthia and Asnani 1982). The channel floor is above 500 m from the mean sea level and has a depth that varies between 610 and 1524 m, and a width that varies between about 140–700 km. The channel is approximately 700 km long and is oriented from southeast to northwest connecting northwestern Kenya to southwestern Sudan. Kinuthia and Asnani (1982), and Kinuthia (1992) observed the presence of the Turkana low-level jet in this valley. The channel is wider at the center as compared to the entrance and the exit. Lake Turkana lies in the middle part of this channel at approximately latitudes 35.5° and 36.5°E and longitudes 2° and 4°N (Fig. 1).

During the months of May–September, the south-

easterly (SE) monsoon flow dominates over the eastern and the coastal parts of East Africa. This north–south monsoon flow is associated with the East African low-level jet (EALLJ). This jetstream is one of the major well-recognized cross-equatorial flows that have been studied through theoretical and numerical models (Findlater 1966; Anderson 1976; Krishnamurti et al. 1976; Findlater 1977; Ardanuy 1979; Bannon 1979; among others). The jet core is generally located between 1 and 1.6 km above the mean sea level and is associated with flows across the equator carrying Southern Hemisphere air northward up the African continent and ending at the Indian subcontinent. This jet stream induces strong currents and upwelling over the western equatorial Indian Ocean. It thus plays an integral role in the seasonal development of the Somali Current, an intense ocean current, which flows northward only during the southwest monsoon but whose strength then is comparable to that of the Gulf Stream over the eastern coast of the United States of America (Anderson 1976). The jet builds during the months of April and May and decays in September and October, during which the flow reverses to northeasterly (NE) monsoons.

Kinuthia and Asnani (1982) and Kinuthia (1992) observed that throughout the year the NE and SE monsoons air near the equator, branches off from the Indian Ocean enters the Turkana channel and intensifies into the Turkana easterly low-level jet. Kinuthia and Asnani (1982) further postulated that the configuration of the Ethiopian highlands and the East African highlands could be playing a critical role in the development and maintenance of the Turkana low-level jet through the orographic channeling effect. This phenomenon has not been fully understood. Previous studies, (e.g. Krishnamurti et al. 1976; Ngara and Asnani 1978) have also indicated the importance of orography on the EALLJ. Krishnamurti et al. (1976) investigated the role of the Ethiopian highlands, the East African highlands, and the Madagascar Mountains on the East African low-level Jet. Their results showed that the Ethiopian and the East African highlands are crucial for the observed strong winds off the coast of Somalia while the Madagascar Mountains are most important for the strong winds just downstream from Madagascar.

Most of the East African region receives two distinct rainfall peaks during the months of March to May (''long rains'') and October to December (''short rains''). The rainy months coincide with the transition of the monsoons during the time when the cross-equatorial flow is weak, more easterly. During the monsoon months the low-level winds are relatively strong and are rather divergent, resulting into generally lower rainfall amounts over the East African coast than farther inland. The northern and eastern parts of Kenya including the Turkana valley are semiarid, and receive an estimated annual rainfall of less that 500 mm as compared to the East African and the Ethiopian highlands that receive over 1000 mm of rainfall annually. In the Turkana channel lies the Chalbi Desert, which is 150 km long and situated from 2°35′N to 3°20′N and from 37°00′E to 37°50′E. This desert region extends from southeast to northwest to join the Koroli Desert to the south. These desert regions stretch from southeast to northwest as the direction of the prevailing wind flow over the channel and are located near Lake Turkana, which lies in the wider part of the valley (Fig. 1). Recent studies by Patwardhan and Asnani (1999) have indicated the importance of orographic channeling in determining the mesoscale rainfall distribution observed over a mountain gap of India. In this study we investigate the role of the Turkana channel in determining the observed climatic conditions over the middle and wider parts of the valley.

1) The Turkana low-level jet

Ever since the discovery of a skeleton related to human evolution by Dr. Leakey in the Turkana channel, many archeological expeditions continue to be carried out in this valley. Pilots flying here occasionally experience strong winds associated with severe turbulence during takeoff and landing. A number of aircraft accidents have been reported in the valley of recent years, which calls for need to understand the dynamics of the flow patterns in the valley in order to identify areas associated with strong winds for aviation safety. There is also need to investigate the causes of the observed semi-arid climates in this valley.

Various criteria have been used to classify the low-level jets (LLJ). Stull (1988) defined the LLJ as occurring whenever there is a relative wind speed maximum that is more than 2 m s^{-1} faster than wind speeds above it within the lowest 1500-m of the atmosphere. Chen et al. (1994) classified the LLJ into two categories: the boundary layer jet (BLJ), which occurs in the Planetary Boundary Layer (PBL) with very strong vertical wind shear and shows a remarkable diurnal variation reaching maximum intensity by early morning and breaking down in the afternoon and, the LLJ, which occurs between 600- and 900-hPa levels, usually associated with synoptic-scale systems. The Turkana jet has been observed to exhibits strong diurnal variations (Kinuthia and Asnani 1982; Kinuthia 1992) and is associated with the synoptic-scale cross-equatorial monsoon flow, both of these phenomena are included in the definition of a LLJ by Chen et al. (1994).

The main observed features of the Turkana easterly low-level jet according to Kinuthia and Asnani (1982), and Kinuthia (1992) are

1) the existence of strong winds within the channel throughout the year with the speeds decreasing in regions where the channel becomes wide;
2) the existence of two distinct jetstreams, detached from each other, throughout the channel except at the middle of the channel where they seem to combine into a single and very high jet;

3) the level of maximum wind occurs in the layer 305–2438 m;
4) general backing of the mean wind to the east and northeast aloft throughout the channel;
5) a maximum wind of about 26 knots ($\sim$13 m s^{-1}) near the channel entrance during the boreal winter season. Winds stronger that 40 knots ($\sim$20 m s^{-1}) have been observed occasionally during this season.

Some scientific questions that are still unanswered on the jet are 1) what role the large-scale orographic forcing plays in its formation and maintenance, 2) whether the depth of the channel is important in determining the vertical structure of this jet, 3) what role is played by the cross-equatorial monsoon in determining the strength of the jet and, 4) whether thermal effects play any significant role on the jet or is this purely mechanical channeling that is important.

2) HYPOTHESIS OF FORMATION AND MAINTENANCE OF TURKANA LOW-LEVEL JET

We hypothesize that some of the scientific questions listed above are important in the formation and maintenance of the jet. The orography over East African highlands and the Ethiopian highlands may be important in providing a valley suitable for the channeling of the monsoon wind system. The presence and strength of the large-scale monsoon flow may be crucial in maintaining the strength in the jet cores and, the depth of the channel may play a role in determining the vertical extent of the jet cores and the total mass transfer along the channel. In the present study, we do not consider the other possible effects such as the air–sea interactions, detailed boundary layer dynamics, detailed vertical resolution or possible effects of the middle latitude interactions that may be important to the Turkana jet. In this study, we shall be primarily concerned with the problem of the numerical simulation and analysis of the impacts of orography and other possible forcing mechanisms (large-scale monsoon and the depth of the channel) on some of the observed features of the jet.

Kinuthia and Asnani (1982) and Kinuthia (1992) have alluded that orographic channeling effect may be responsible for the Turkana low-level jet. The dynamics of the channeling effects could be explained through the application of the Bernoulli equation for barotropic [$\rho = \rho(p)$] flows derived from a modified Eulerian equation of the form

$$\frac{DR}{DT} = \frac{1}{\rho}\frac{\partial p}{\partial t} + \mathbf{u}\cdot\mathbf{F} + \frac{p}{\rho^2}\dot{H}, \tag{1}$$

where the Bernoulli function, R is defined by

$$R(x, y, z, t) = \frac{1}{2}q^2 + gz + \frac{p}{\rho}, \tag{2}$$

where $q^2 = u^2 + v^2$, u, v are east–west and north–south components of horizontal wind, g the gravitational acceleration, z the height above mean sea level (AMSL), p is the pressure, ρ the air density, and $\mathbf{F}$ and H represent internal processes, such as turbulence or viscous effects, or external ones such as additional body forces or radiative heating. Here H (kg m^3 s^{-1}) represents some heating process that may affect the density without changing the total mass. In a steady flow without forcing or heating, R is constant along a streamline. On the other hand, if the fluid passes through a region where there are significant frictional or turbulent stresses (represented by $\mathbf{F}$) like the rough sides of the mountain valleys, then the flow on each streamline would be affected by these stresses, which will reduce R. When the flow is constrained to a channel, as in straits, the effect of rotation in the down stream direction can be small, even at quite large distances (Baines 1995). Viscous forces are dominant close to the rough walls and at the bottom of the channel and are insignificant away from these surfaces. Hence, if we consider an inviscid, steady, irrotational, barotropic flow and neglect the viscous forces then

$$R = \frac{1}{2}q^2 + gz + \frac{p}{\rho} = \text{constant everywhere.} \tag{3}$$

The first term on the right-hand side of Eq. (3) represents the total kinetic energy while the remaining two terms represents the total potential energy. The term p/ρ represents the contribution by the dynamic pressure to the total potential energy. Thus, under simplified assumptions, Bernoulli's theorem may be stated as follows: under steady-state conditions, a fluid mass flowing horizontally conserves the sum of its potential and kinetic energy. When the boundary conditions constrain the fluid to pass from a narrow cross-section to a wider cross-section, then its velocity decreases, kinetic energy decreases, and potential energy in the form of pressure increases; this increase of pressure is called dynamic pressure (Patwardhan and Asnani 1999). Consequently, the mass flow rate across the channel can be approximated by

$$M = \rho A(2gh)^{1/2}, \tag{4}$$

where A is the area at the channel entrance and h is height AMSL. In this study we use the Bernoulli theorem to have a better understanding of the flow in the Turkana channel.

2. The regional climate model

In this study, we explore the use of a regional climate model, capable of distinguishing between the primary geographical climate anomaly regimes over East Africa, a region where the local forcings have been identified as a major contributor to climate (Okeyo 1986; Mukabana and Pielke 1996; Nicholson 1996).

a. A brief description of the numerical model

The model used in this study is the second-generation RegCM. Giorgi et al. (1993a,b), Kiehl et al. (1998) and Sun et al. (1999a,b) have discussed details regarding the various attributes of the RegCM and its customization to the East African region. This climate model is based on the primitive equations and a terrain-following (σ) vertical coordinate system. The model vertical structure includes 16σ levels with the model top at 50-mb and six levels are below $\sigma = 0.79$ level. The model domain size is 5580 km $\times$ 5040 km centered at 4°S, 31°E, and a horizontal grid spacing of 60 km.

1) Model physics: Interactive biosphere atmosphere transfer schemes (BATS), that represent the role of vegetation and interactive soil moisture that modifies the surface–atmosphere exchanges of momentum, energy, and water vapor is used. The BATS scheme has been found to perform better in this climate model (Giorgi and Marinucci 1991; Giorgi et al. 1993b) and over the East African region in particular (Sun et al. 1999). In the PBL formulation, for stable planetary boundary layer, the heat, moisture, and momentum fluxes are estimated using the first-order K-theory. For the convective boundary layer calculations, the nonlocal eddy diffusion formulation of Holtslag et al. (1990) is used. Two schemes are available for the generation of precipitation in the RegCM. An implicit scheme, whereby supersaturated water immediately precipitates or explicit scheme including prognostic equations for cloud-water and rainwater (Hsie et al. 1984) describes nonconvective precipitation. Convective precipitation is described as the Grell scheme (Grell 1993). The scheme is activated when a parcel lifted from the updraft originating level eventually attains moist convection. Sun et al. (1999) have indicated that the Grell cumulus schemes yields better results than the Kuo scheme over the equatorial eastern African region perhaps because it responds more readily to variations in tropical atmospheric stability conditions. For more detailed analysis of the parameterization schemes and their influence on the model results, the reader is referred to the earlier works by Giorgi et al. (1993b) and Sun et al. (1999).
2) Boundary conditions: Orography is incorporated in the model as the lower boundary condition in a terrain-following vertical coordinate system. Pressure has been widely used as a vertical coordinate in modeling and theoretical studies ever since the pioneering work by Eliassen (1949). Using pressure as an independent variable eliminates the not routinely observed air density from the governing equations and simplifies thermodynamic calculations. Furthermore, numerical models in such a coordinate system can easily incorporate observational data that are generally available at pressure levels (Xue and Thorpe 1991). There are, however, deficiencies of the sigma treatment of orography. This scheme may not handle sharp terrain gradients effectively. The orography data used in this study was taken from the global 5′ horizontal resolution orography file archived at International Research Institute. This data was interpolated to the model horizontal grid resolution of 60-km using the Cressman interpolation scheme (Cressman 1979). At this resolution, the main features of the bottom topography are well resolved over eastern Africa (Fig. 1). The land-use data adopted in the model was interpolated from 30′ resolution data archived at National Centers for Atmospheric Research (NCAR). The time-dependent sea surface temperature (SST) was interpolated from a 1° $\times$ 1° grid of the monthly mean observed data (Shea et al. 1992). The lateral boundary conditions were constructed based on the relaxation method developed by Anthes et al. (1987), and Giorgi et al. (1993b). These conditions were prescribed at every 1200 LST of integration using the European Center for Medium Range Weather Forecasts (ECMWF) reanalysis data. In principal, the replacement of the new GCM boundary conditions should be made at each time step, but studies by Kida et al. (1991) has shown that the error introduced by 12-hourly lateral boundary updates is negligible. The ECMWF reanalysis data is based on T42 spectral grid that corresponds to about 2.8° $\times$ 2.8° horizontal resolution in physical space and is available on 14 pressure levels. No further adjustments were done to the initial and boundary conditions although the spatial interpolation to our model resolution may introduce slight imbalance. Many researchers (Murakami and Sumathipala 1989; Mukabana and Pielke 1996; Okoola 1999, among others) have utilized ECMWF datasets for various studies and have found the datasets to give reasonable approximations of the flow fields over eastern Africa and the Indian Ocean.
3) Initial conditions: Initial conditions in a numerical simulation represent the mean space-time characteristics of the atmosphere at the beginning of the numerical experiment. The model was initialized with the 1200 LST ECMWF reanalysis meteorological fields for the first day of September 1988. The initial conditions in this climate model are used to start the model integrations and are not expected to influence the final simulations (e.g., Giorgi and Mearns 1999). Studies by Giorgi et al. (1993a) have discussed in depth the RegCM development and have addressed some aspects of the model sensitivity to physical parameterization and choice of domain. Sun et al. (1999a) tested different domain sizes in the customization of the RegCM to the East African region. In this study we have adopted the model domain similar to that used in Sun et al. (1999b). The simulation period was September through December coinciding with the short rainy season over eastern Africa. The first month (September) results were discarded to

allow for the model to spin-up. The year 1988 that displayed near-normal rainfall conditions (Ininda 1998; Sun et al. 1999b) was used in our control runs. Model results were analyzed at 1200 and 2400 LST. Multiple simulations starting from slightly perturbed initial conditions were performed to provide input for the computation of ensemble statistics for assessing the averages and spread of the forecasts.

b. Design of numerical experiments

In order to test our hypotheses, a series of numerical experiments were designed to explore the relative importance of each of the three parameters (orography, large-scale monsoon flow, and depth of the channel) in the formation of the Turkana LLJ.

1) Experiment 1: all forcing mechanisms were incorporated in the domain (hereafter referred to as Control).
2) Experiment 2: the entire bottom topography was reduced to the 500 m AMSL (the lowest level of the channel depth) over the model domain and the large-scale wind remained the same as in Experiment 1. Hence, there was no channel in this experiment. The purpose of this experiment is to investigate the role of large-scale orography and the presence of the valley in the formation and maintenance of the jet.
3) Experiment 3: the model was started from rest ($u = v = 0$) to eliminate the impact of the large-scale monsoon wind flow. Orography and channel depths were kept the same as in Experiment 1. The purpose of this experiment is to find out the importance of large-scale forcing in the realistic simulation of the jet. By eliminating the large-scale forcing, it is also possible to investigate the combined impacts of thermal heating and surface drag on the jet. The effects of thermal heating, frictional drag, and the pressure gradients are the major forcing mechanisms still present in the large-scale when the model integrations are started from rest.
4) Experiment 4: the bottom of the Turkana channel was artificially raised up to a mean depth of 1000 m AMSL. The large-scale forcing fields were kept the same as in Experiment 1. The purpose of this experiment is to investigate the role of the channel depth on the jet development and strength.

By performing these experiments, we anticipate to have a better understanding of 1) the role each of these three factors (orography, large-scale monsoon wind, and depth of the channel) in the formation and variation of the jet, and 2) the cross-sectional temperature distribution in the core of the jet, and 3) the observed semiarid climates over the Lake Turkana basin.

3. Model results and discussion

Results of numerical experiments conducted in this study are discussed in this section. The four series of experiments are presented independently below.

a. Model results of the control run

This section highlights the major features that were observed with the control model experiment. The simulated wind vectors for November are shown in Fig. 2a. The data over the shaded highland areas that has the surface above 1500 m may not be realistic. The large-scale monsoon flow during this section emanates from a high-pressure cell located over the Arabian peninsular and the Mascarene anticyclone located in the southern Indian Ocean. Northeasterly to northerly flow is simulated at 850-hPa level over the eastern parts of the domain north of 6°S. The wind is convergent over the western parts of Tanzania and the costal regions. The wind over the coastal regions is rather divergent. Winds stronger than 7 m s^{-1} are simulated over the eastern lowlands and the Turkana channel, while relatively weaker winds of about 4 m s^{-1} are simulated over the western highlands of East Africa including the Lake Victoria basin (Fig. 3).

The flow at 700 hPa (Fig. 2b) is more easterly along the Indian Ocean coast. At this level, the meridional flow corresponding to the northeast monsoon switches to a quasi-easterly flow, advecting moisture from the Indian Ocean to the inland areas (Camberlin and Wairoto 1997). There is an indication of wind convergence over the Eastern Highlands of Kenya and northwestern Tanzania. These convergence zones is linked to interaction between the mesoscale land/sea breeze and anabatic/katabatic flows, and large-scale mean monsoon flow (Mukabana and Pielke 1996; Indeje and Anyamba 1998).

Simulated and reanalysis surface temperature fields (figure not shown) shows isotherms that display an alignment following the terrain over the region. Higher temperatures (greater than 27°C) are simulated over the Indian Ocean coast, Lake Victoria basin, and over Lake Tanganyika. Temperatures lower than 18°C are shown over the East African and Ethiopian highlands. Higher temperatures are also shown over the semidesert areas of northeastern Kenya and central Tanzania. Specific humidity values higher than 14 g kg^{-1} are simulated over the East African highlands and the Lakes Victoria and Tanzania and values lower than 10 g kg^{-1} are simulated over the hot and dry semiarid areas in the region including the Turkana channel (figure not shown). Extensive verification of the model in reproducing the mean climate over East Africa is reported in the papers by Sun et al. (1999b).

b. Simulation of the Turkana low-level jet

Model simulation results for the 1988 season are reported in this section. The simulated characteristics of the jet are compared with the limited observations that were carried out in the channel by Kinuthia (1992) during the month of February 1983. These are the only

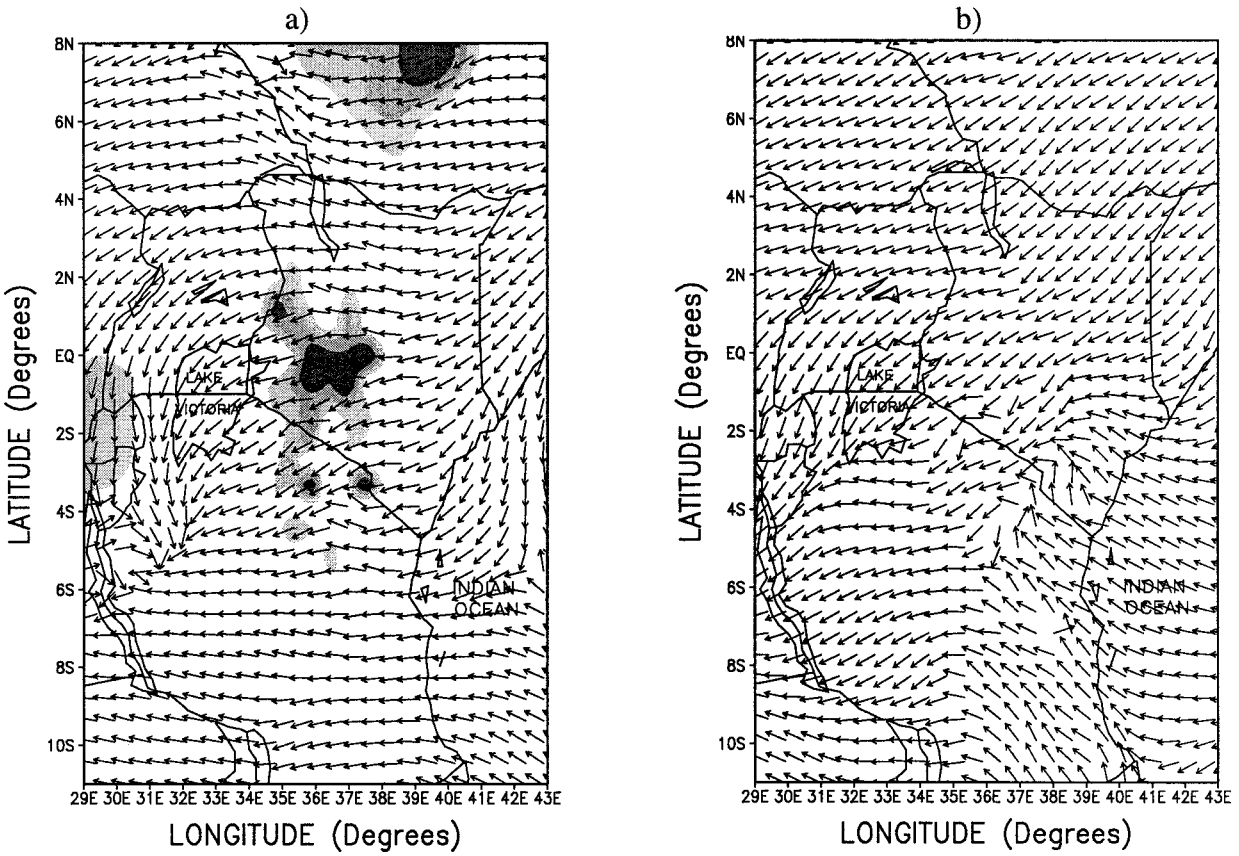

FIG. 2. Simulated Nov mean horizontal wind vectors at (a) 850-hPa and (b) 700-hPa levels. Shaded are region where the surface terrain is above 1500 m AMSL.

available observations, which is close to the boreal winter season considered in this study.

1) MODEL CONTROL RUN

In this subsection, results from the control model run are further analyzed. Orography and other forcing mechanisms (large-scale flow and depth of the channel) are incorporated in these experiments. In Kinuthia and Asnani (1982), and Kinuthia (1992) observational analysis, they found the Turkana low-level jet to exist throughout the year but only varied in intensity from season to season. We chose to study the features of the jet during the months of November because the model we are using has only been customized and tested for the region during the October to December season (Sun et al. 1999a). We, however, recommended that similar studies be carried out during the months of June–July when the cross-equatorial monsoon flow is strongest and the Turkana low-level jet is expected to be at its maximum.

Figure 4 illustrates the simulated flow patterns in the Turkana channel during the northeast monsoon period of November. Streamlines at 950-hPa level show southeasterly to northeasterly flow before entering the channel. On entering the channel, the streamlines become confluent and turn to southeasterly. Convergent wind is shown at the channel entrance and exit while divergent wind is indicated at the middle of the channel. Fanning-out like streamlines are shown as the flow exits the valley. These model results agree with the observational studies reported by Kinuthia (1992). Ramachandran et al. (1980) also observed a fanning out of surface winds as they emerged from a mountain gap over India. Our results indicate that the flow becomes diffluent in the middle and wider part of the channel, and becomes confluent at the jet exit as the channel becomes narrower again. Kinuthia (1992) observed similar characteristics associated with this jet.

The latitude–height cross section of mean horizontal wind speed for October, November, and December along the channel is shown in Figs. 5a, b, and c, respectively. The mean wind flow below 750-hPa level over the eastern parts of the channel is mainly southeasterly during the month of October and varies between southeasterly and northeasterly in November and December. This flow extends from surface to about 800-hPa level were it becomes predominantly easterly. Above 700-hPa level, the flow is mainly northeasterly as shown during the months of November and December. Transition of the mean wind to the east and northeast aloft throughout

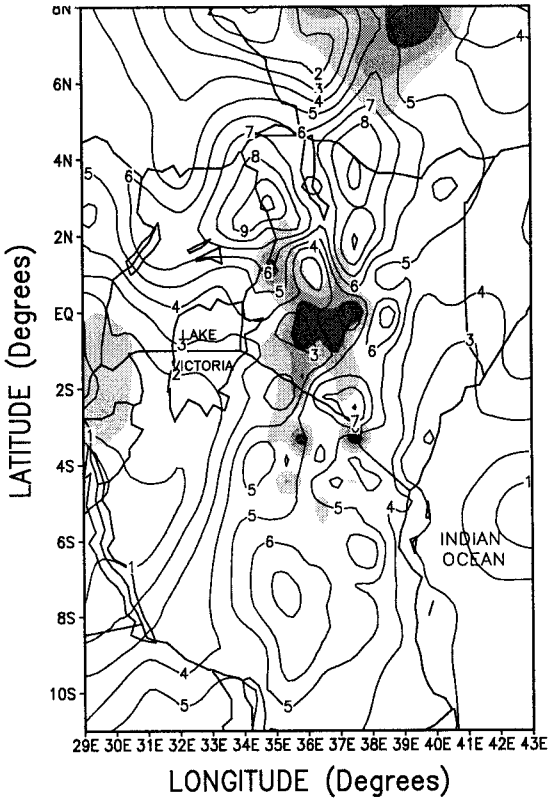

FIG. 3. Simulated Nov mean horizontal wind speed at 850-hPa level. Shaded are areas of terrain height above 1500 m AMSL.

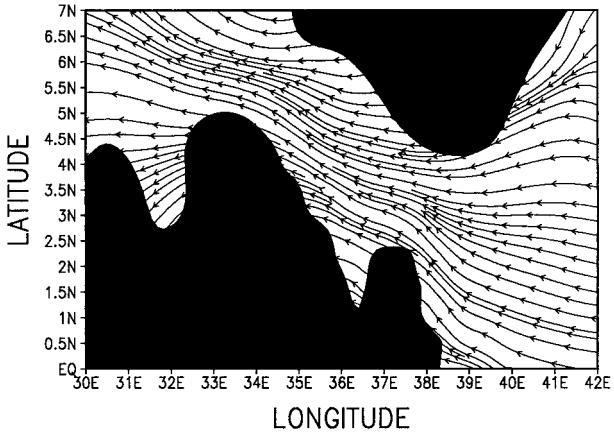

FIG. 4. Streamlines of the simulated Nov mean conditions at 950-hPa level over the Turkana channel in the control run. Blackened areas are regions where the surface terrain is above 1000 m AMSL.

the channel is also indicated during the months of October and November. The level of maximum winds occurs in the layers 930-hPa and 650-hPa. The levels of maximum winds are shown declined down from the entrance to the middle region and then rise up again toward the exit during October (Fig. 5b). The level of maximum winds at the entrance of the channel is about 900–950 hPa and the exit is about 850- to 825-hPa levels for the three months. In the middle of the channel the jet cores are shown to combine into one single jet centered at 700-hPa level (especially in November). The southeasterlies and the easterlies increase in intensity throughout the channel, and from the surface to the level of the occurrence of mean maximum wind, then decreases aloft. The largest value of the mean maximum wind speed in the jet cores is about 11 m s^{-1} (~22 kt).

The jet is weaker in October and intensifies in November and December to almost twice the speeds observed in October. Weakening of the winds in the middle of the channel to about a half the values observed at the entrance and exit could be due to the widening of the channel width in that section. This observation is supported by the Bernoulli Eq. (3) whereby the potential energy in the form of dynamic pressure rises at the wider part of the channel resulting in a decrease in the kinetic energy and slowing down of the winds. The observed increase in the wind speed at the channel exit may be explained in terms of (a) narrowing of the channel from the center toward the exit and, (b) a conversion of potential energy to kinetic energy that may occur [supported by Bernoulli Eq. (3)]. Baines (1995) has also given broader discussion of the energy conversions associated with flows exiting a valley.

2) EFFECTS OF LARGE-SCALE OROGRAPHY ON THE JET

We intend to ignore the spatial variation of orography in this case study with all other parameters remaining the same. The solution of the streamlines at 850-hPa level in November for this experiment (figure not shown) are generally northeasterly throughout the channel and the observed southeasterly flow in the channel is missing. Figure 6 shows the wind vectors and isotachs. When compared with Fig. 5, the wind speed in this case is weak with a maximum of about 6 m s^{-1} over the channel and the jet cores are either missing or very unrealistic. There is also small variation of wind speed with height. The observed strong winds are not present in the jet cores at the entrance and exit of the channel. These results generally indicate missing of the key features associated with the jet when the entire topography is suppressed. These results indicate the importance of the large-scale orography for the simulation of the Turkana jet.

3) INFLUENCE OF THE LARGE-SCALE MONSOON FLOW ON THE JET

Sensitivity of the Turkana low-level jet to the clam wind speed is investigated in this case study by initializing the model with no (zero) ambient wind ($u = v = 0$). The large-scale kinematics forcing at the lateral boundaries was also set equal to zero throughout the simulation. Figure 7 shows the results from these experiments. The wind flow over the channel turns from

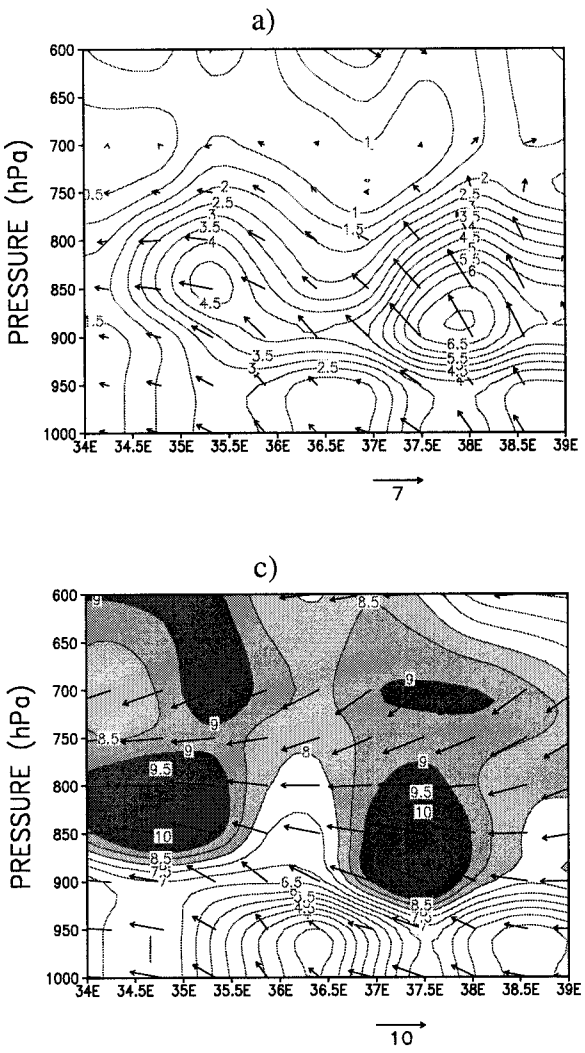

FIG. 5. Simulated mean horizontal wind speed for (a) Oct, (b) Nov, and (c) Dec at lat. 3.5°N along the Turkana Channel in the control run. Shaded are values with wind stronger than 8 m s^{-1} and vectors indicate the wind speed and direction.

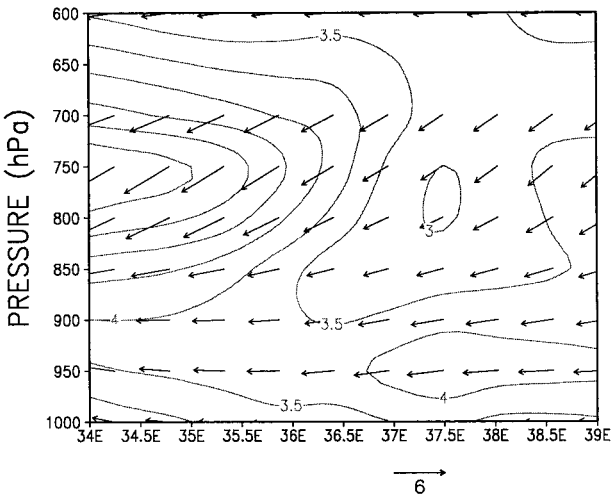

FIG. 6. Simulated Nov mean wind speed along the Turkana channel, for the NOTOPO experiment. Vectors indicate the wind speed and direction.

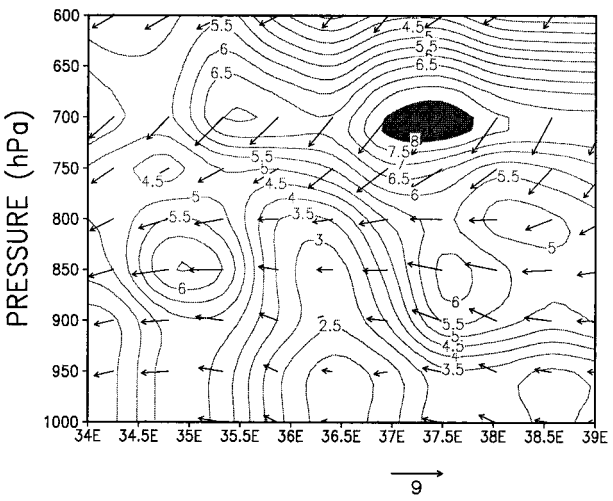

FIG. 7. Simulated Nov mean wind speed along the Turkana channel, for the zero large-scale ambient wind experiment. Vectors indicate the wind speed and direction.

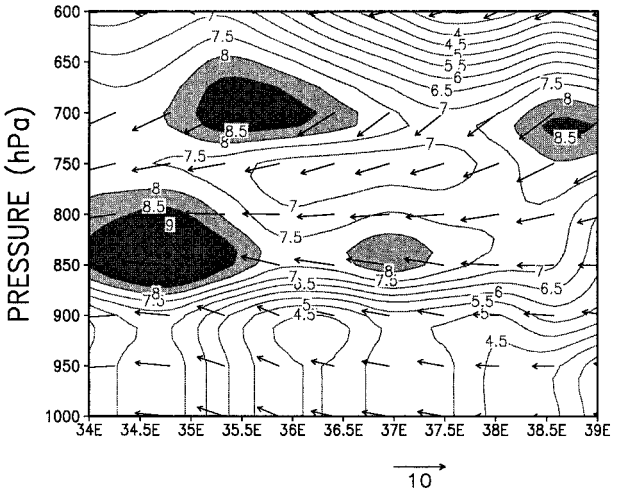

FIG. 8. Simulated Nov mean wind speed along the Turkana channel, for the channel depth experiment. Vectors indicate the wind speed and direction.

northeasterly to southeasterly at the channel entrance (figure not shown). These streamline analyses compare well with results in the control run. The tendency of the wind speed to increase with height throughout the channel is also observed (Fig. 7). However, the maximum wind speed in the jet cores is about 6 m s^{-1} at the valley entrance and exit, and about 9 m s^{-1} at the middle of the valley centered at about 700-hPa level. Compared to the control simulation, the winds in this case are weaker by 50%. These results indicate that the large-scale flow enhances the strength of the wind speed in the jet cores. Thermal forcing and possibly the effect of surface drag in concentrating the flow along the jet core may play equal roles as that of the large-scale monsoon in the development and maintenance of the Turkana low-level jet. These results show the existence of weaker jet cores (by about 50% of the mean) during the periods of weak large-scale monsoon flow.

4) EFFECTS OF THE CHANNEL DEPTH ON THE TURKANA JET

In this experiment the large-scale orography and the large-scale monsoon flow are included and the depth of the channel was artificially raised to a constant level of 1000 m AMSL. The channel depth plays a role in balancing the kinetic/potential energy in the channel as shown in Eq. (3). The channel depth is also important in regulating the mass flow across the channel indicated in Eq. (4). Results obtained from this simulation are depicted in Fig. 8. There is reduced streamline convergence over the channel. The jet cores tend to combine and move to the center of the channel where strong winds (~7 m s^{-1}) are shown. There is also a general rising in the level of the jet cores to center at about 850- and 650-hPa levels. These results indicate that the depth of the channel plays a role in determining the correct height of the observed jet cores in the Turkana easterly low-level jet.

c. Mechanisms controlling climate in the Turkana channel

In this section we investigate the mechanisms responsible for the observed climate variability over different parts of the Turkana channel.

1) DIVERGENCE, VERTICAL MOTION, AND VORTICITY

The horizontal wind divergence was computed for the entrance, middle, and exit of the channel and the results are shown in Fig. 9. These results indicate that at the entrance and the channel exit, convergence (~1.0 $\times 10^{-5}$ s^{-1}) occurs below 900-hPa level and divergence (~0.3 $\times 10^{-5}$ s^{-1}) between 860- and 760-hPa levels. In the middle of the channel, relatively weak horizontal wind divergence (~0.2 $\times 10^{-5}$ s^{-1}) is indicated below

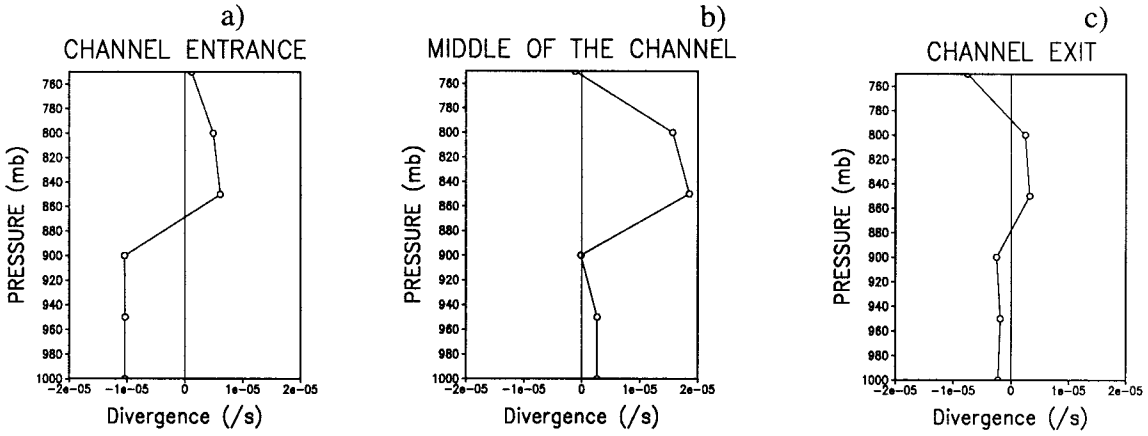

FIG. 9. Simulated Nov mean horizontal divergence at (a) the channel entrance near Marsabit, (b) middle of the channel around Lake Turkana, and (c) at the exit of the channel near Logichoggio, for the control model run. These locations are shown in Fig. 1.

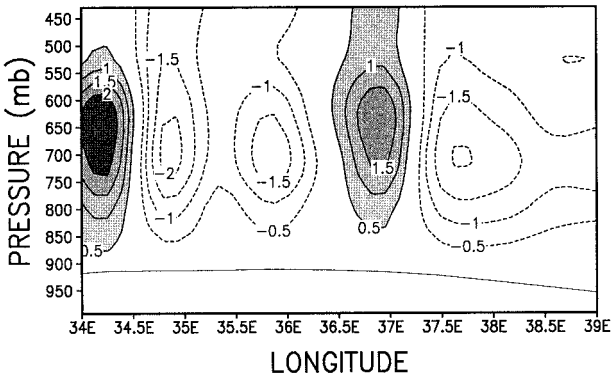

FIG. 10. Longitude–height cross section of vertical velocity at lat 3.5°N along the Turkana channel. Shaded are areas of upward vertical velocity. The bottom orography, which is almost flat in the channel, is also shown.

900-hPa level and increase to a maximum of about 1.8 $\times 10^{-5}$ s^{-1} located at 860-hPa level followed by a general decrease aloft. The observed low-level horizontal divergence in the middle of the channel and over the Lake Turkana basin may inhibit any convection associated with the mesoscale circulation around the lake basin. Several studies have shown these areas to display arid to semi-arid climates (Ogallo 1980; Indeje et al. 2000).

These results of divergence/convergence fields are consistent with those obtained from the observational and analytical studies by Kinuthia (1992). The low-level horizontal wind divergence in the middle of the channel partly explains the splitting of the jet cores at these parts of the valley. Consequently, convergence of the horizontal wind above 750-hPa level explains the reappearance of a combined jet at 700-hPa level in this part of the channel. Previous studies have shown similar phenomenon in barotropic flows (Thompson 1957; Wiin-Nielsen 1961; Krishnamurti et al. 1976; and others). Krishnamurti et al. (1976) have associated strong divergence in the flux of westerly momentum to the splitting of the East African low-level jet (EALLJ) observed over the western Indian Ocean during the period May–October. Regions of large net divergence of easterly momentum flux may result in the weakening of a parent Turkana jet and a new jet may form in the vicinity where there is large net convergence of easterly flux of momentum.

Figure 10 shows the longitude–height cross section of vertical velocity along the Turkana Channel. Centers of upward/downward vertical velocity are located between 850- and 500-hPa levels. Downward vertical motion of about 2.0 $\times 10^{-2}$ m s^{-1} is shown before the channel entrance located at 37.5°–38°E. This downward motion can be related to the divergent nature of the easterly monsoon flow in the low levels (Lumb 1966). Upward vertical motion ($\sim$1.5 $\times 10^{-2}$ m s^{-1}) is simulated at the channel entrance (centered at 37°E), and at the exit of the channel, it is about 2.5 $\times 10^{-2}$ m s^{-1} (located between 34° and 34.5°E). In the middle of the channel and over the Lake Turkana basin (between 34.5° and 36.5°E), downward vertical motion is dominant with two centers of about 2.0 $\times 10^{-2}$ m s^{-1} as indicated in Fig. 10. The dominant downward motion over the Lake Turkana basin could inhibit any convective activity and thus weakening any development of the mesoscale circulations over this region. The vertical motion field in the channel is consistent with the simulated horizontal divergence field (Fig. 9). Upward/downward motion is associated with low-level convergence/divergence zones. The vertical velocity fields over different parts of the channel are consistent with the Bernoulli theorem [Eq. (3)]. Because of the strong winds at the entrance and exit of the channel, the kinetic energy term is large and hence the dynamic pressure term must be low in order to keep the energy balance in the flow. The resulting decrease in the dynamic pressure is conducive for the upward vertical motion shown at the entrance and exit of the channel. Likewise, the kinetic energy term in Eq. (3) is low in the middle of the channel and the dynamic pressure is high resulting in downward motion indicated over these areas.

Vorticity of mean winds at the channel entrance, middle, and exit is shown in Fig. 11. At the channel entrance anticyclonic vorticity is simulated above 950-hPa level with a maximum ($\sim$2.0 $\times 10^{-5}$ s^{-1}) shown at 900-hPa level. In the middle of the channel, anticyclonic vorticity is simulated below and above 900-hPa level and cyclonic vorticity indicated at 900-hPa level. The anticyclonic vortices that exists at the entrance and middle of the channel is possibly due to the friction effects that slow down the southeasterly to northeasterly currents along the mountain edges. Kinuthia (1992) observed that the anticyclonic relative vorticity existed in the northern half and cyclonic relative vorticity in the southern half over the eastern parts of the channel. At the exit of the channel, relatively weak anticyclonic/cyclonic vortex is shown. This may indicate that the flow is nearly irrotational at the section. Also, at the channel exit the vortices could decay unless they receive some energy to sustain them. Kinuthia (1992) postulated that the vortices generated in the Turkana channel may contribute to the midtropospheric African Easterly jet associated with the easterly waves over West Africa that ultimately develop into hurricanes observed over the eastern coast of the United States of America.

2) TEMPERATURE AND MOISTURE STRUCTURE IN THE VALLEY

Figure 12 shows the mean temperature at 850-hPa level over the Turkana channel for the month of November. The figure indicates a nearly homogeneous temperature along the channel. High temperatures (>18.5°C) are indicated close to the edges of the valleys, which are exposed more to the solar radiation than the valleys below. In this valley these thermally induced

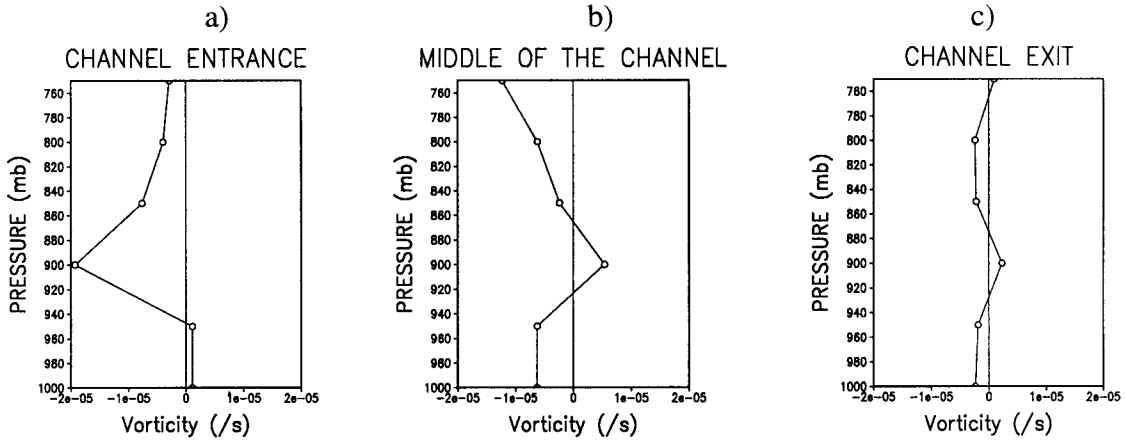

FIG. 11. Simulated Nov mean vorticity at (a) the channel entrance near Marsabit, (b) middle of the channel around Lake Turkana, and (c) at the exit of the channel near Logichoggio, for the control model run.

flows are cross wind to the Turkana jet axis and are likely to be suppressed by the presence of the jet. With a near homogeneous temperature along the channel, one would expect the existence of a weak temperature gradient. This suggests that orographic channeling effects dominate the thermal forcing in the development of this jet. However, low temperatures (~16°C) are indicated over the eastern end of the channel and high temperatures of about 20°C over the western sector of the channel. The temperature difference of 4°C between the two ends of the valley is favorable for the generation of an east–west pressure gradient that could sustain the east to west wind flow along the channel. The constant temperature field along the channel justifies our assumption that the flow is nearly barotropic in this valley.

To study the evolution of water vapor distribution in the channel, the moisture flux divergence was computed using the following equation:

$$F_V = \nabla \cdot (q\mathbf{V}). \tag{5}$$

Here, F_V was multiplied by minus one for convenience.

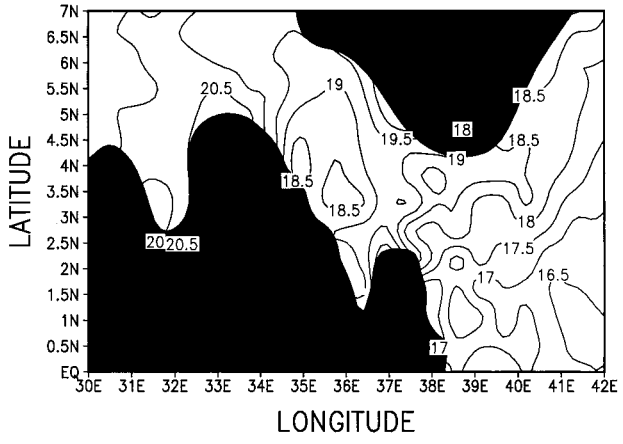

FIG. 12. Simulated Nov mean temperature (°C) at 850-hPa level over the Turkana channel in the control model run.

Thus, $F_V < 0$ indicates moisture flux divergence and $F_V > 0$ indicate moisture flux convergence. Moisture flux divergence fields combine the horizontal advection of moisture with mass convergence, which are the two prime factors in developing strong convection (Doswell 1977). Areas of increasing moisture contribute to destabilization, while mass convergence results in vertical motion. The forcing and destabilization resulting from moisture convergence may be used to diagnose areas of convection. Equation (5) refers to moisture flux divergence, which would be similar to the vertically integrated moisture flux distribution. The main objective of this paper is not to study a detailed moisture balance across the region as to indicate sources and sinks, but to use the moisture divergence/convergence field to explain the observed dry/wet conditions over parts of the channel.

Figure 13 shows the simulated moisture flux divergence along the Turkana channel. Moisture flux convergence (~4.0×10^{-6} kg kg^{-1} s^{-1}) is indicated over the channel entrance and exit. In the middle of the channel, divergence of moisture flux (~5.0×10^{-6} kg kg^{-1} s^{-1}) is shown. There is a tendency for the centers of the moisture flux convergence/divergence to tilt with height from the channel entrance to the channel exit. The simulated moisture flux divergence over the Lake Turkana basin could further inhibit developments of mesoscale circulations over these areas. Moisture flux convergence/divergence zones compare well with the simulated upward/downward vertical velocity over different parts of the channel and are consistent with the Bernoulli Eq. (3). Sections with upward/downward motions are associated with positive/negative fluxes of moisture.

In order to obtain some information about the fluctuations of temperature fluxes and study their evolution at particular locations in the channel, the following flux divergence equation was used

$$G_V = \nabla \cdot (T\mathbf{V}). \tag{6}$$

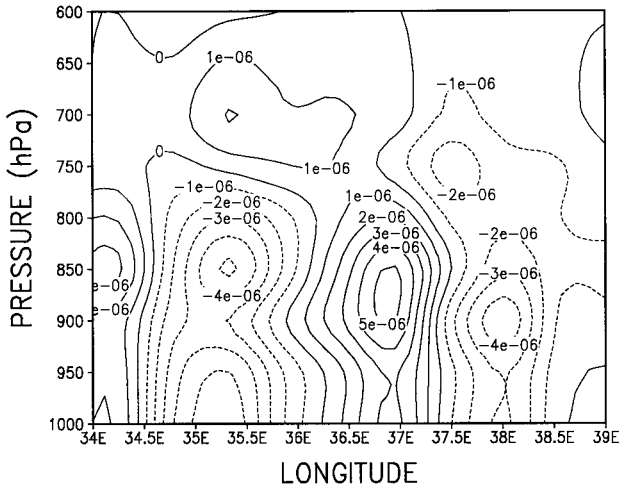

FIG. 13. Simulated Nov mean moisture flux divergence (kg kg^{-1} s^{-1}) along the Turkana channel in the control model run (multiplied by -1). Positive values indicate convergence and negative divergence of moisture flux.

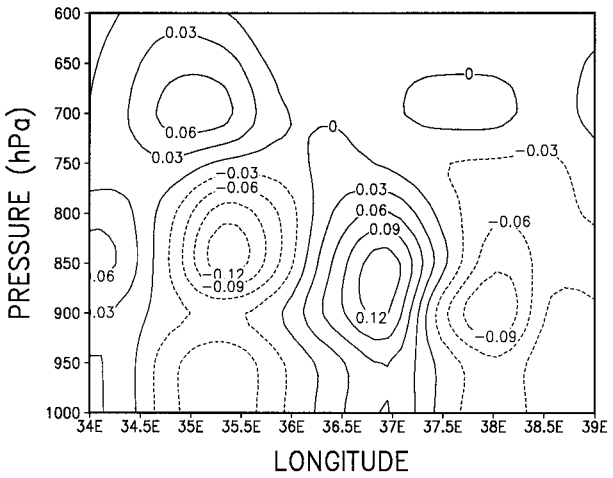

FIG. 14. Simulated Nov mean temperature flux divergence (K s^{-1}) along the Turkana channel in the control model run (multiplied by -1). Positive values indicate convergence and negative divergence of temperature flux.

Here, G_V was multiplied by minus one for convenience. Thus, $G_V < 0$ indicates temperature flux divergence and $G_V > 0$ indicate temperature flux convergence. Figure 14 displays the temperature flux divergence along the Turkana channel. Equation (6) is used to locate regions exhibiting tropospheric warming/cooling within the valley that are conducive for convergence/divergence of moisture fields. We use this approach to reinforce our findings on the physical mechanisms responsible for the wet/dry conditions observed over parts of the Turkana valley.

At the channel entrance and exit, temperature flux convergence ($\sim 12.0 \times 10^{-2}$ K s^{-1}) is indicated. Temperature flux divergence ($\sim 12.0 \times 10^{-2}$ K s^{-1}) is shown at the middle of the channel and to the east of Lake Turkana. The observed cooling of the lower troposphere over the Lake Turkana basin might inhibit convection and cause decreased (moisture) convergence and precipitation. These patterns compare well with the moisture flux convergence and the centers of the jet cores. Based on Eq. (4), if we take the mean depth at the entrance of the channel to be about 1027 m, and the width as 2.5° ($\sim 2.5 \times 111.1 \times 1000$ m), $\rho = 1$ kg m^{-3} and $g = 9.81$ m s^{-2}, then the mass flow rate across the channel is about 3.9×10^7 kg s^{-1}.

d. Summary and conclusions

The NCAR regional climate model (RegCM) was employed to (1) study the kinematics of the Turkana low-level jet that lies between the Ethiopian highlands and the East African highlands, and (2) investigate the mechanisms responsible for the observed dry conditions over the Lake Turkana basin that lies in the wider section of the channel. Series of numerical experiments were conducted to investigate the role played by the large-scale orography and the other two mechanisms namely the large-scale monsoonal background flow and the depth of the Turkana channel to the development and maintenance of the jet. The model results were compared with the observed characteristics of the jet reported in Kinuthia and Asnani (1982) and Kinuthia (1992).

The model was capable of reproducing the observed characteristics of the Turkana easterly low-level jet. Strong winds were indicated in the channel throughout the study period of October to December, with the wind speed decreasing in the middle and wider region of the channel. A split in the jet core was also shown in the middle of the channel. The level of maximum winds occurred in the layers 930-hPa and 650-hPa levels ($\sim$400–3200 m). Kinuthia (1992) reported the existence of maximum winds in the layer between 305 and 2438 m. The highest magnitude of mean maximum wind of 11 m s^{-1} ($\sim$22 kt) was simulated in the channel.

The dynamics of the Turkana channel are explained in terms of the orographic channeling effects associated with the Bernoulli theorem as applied to barotropic steady and nonviscous flows. This study has verified this phenomenon by showing the dependence of the jet on the large-scale orography. Our main results on the forcing mechanisms responsible for the development of the jet can be summarized as follows: (a) orographic forcing is the most important factor, (b) the large-scale monsoon background flow is important in determining the wind speed in the jet cores, (c) the depth of the channel determines the vertical structure and location of the jet cores, and (d) thermal and frictional forcing play equivalent roles as that of the large-scale background winds in the formation and maintenance of the jet. Divergence and anticyclonic vorticity partly explains the observed split in the jet cores in the middle of the channel. Previous studies have shown similar

phenomenon in the low-level jetstreams associated with barotropic flows (Thompson 1957; Wiin-Nielsen 1961; Krishnamurti et al. 1976). This study contributes to a better understanding of the dynamics of the Turkana low-level jet.

The dry condition observed over the Lake Turkana basin are explained in terms of dominant downward vertical velocity, decrease in moisture flux convergence, and increase in temperature flux divergence that inhibit active developments of mesoscale circulations and their interactions with large-scale flow over these areas. These results have also revealed the thermal and moisture structures across the Turkana channel that were not available in the observational studies reported in Kinuthia (1992). There are some physical aspects important for the low-level jets that are not included in this study. Some of these factors include the air–sea interaction over the Indian Ocean that regulate the monsoon flow that ultimately affect the Turkana jet. The temperature difference between the eastern and western ends of the channel could be crucial in initiating the flow across the channel from east to west and needs further investigation. Also detailed study of the surface fluxes of heat, moisture, and momentum in the jet core is highly recommended including a detailed study of the diurnal variations of the jet. This study was done during the months when the easterly monsoon is not at its maximum. A similar study during the period June–August when the large-scale flow is strong is highly recommended. Our model results indicate that the presence of the Turkana low-level jet is a significant climatic feature over the equatorial eastern African region as it plays the role of the ''skeletonal'' structure on which the anatomy of the regional climate of the northeastern Africa evolves. The regions of strong winds associated with the jet are important to the safety in the aviation industry. These regions may also provide alternative energy sources of wind energy since the observational studies have indicated that strong winds exist throughout the year in this valley. Climate-dependent hydropower is the major source of energy in the eastern African region. If wind turbines were installed in areas in the valley with strong winds, then this could provide alternative energy resources. These resources could be used to alleviate the frequently experienced energy shortages that predominate during extremely dry seasons.

Acknowledgments. NSF supported this research work under Grant ATM-9113511. The computations were performed on the North Carolina Supercomputing Center (NCSC) Cray-T90, the *FOAM*^{V} visualization, and parallel computing facility at North Carolina State University, and on the NCAR Cray-T90 supercomputer. NCAR is sponsored by the National Science Foundation. We acknowledge the enlightening discussions with George Pouliot and his help during the various stages of this work.

REFERENCES

Anderson, D. L. T., 1976: The low-level jet as a western boundary current. *Mon. Wea. Rev.,* **104,** 907–921.

Anthes, R. A., E. Y. Hsie, and Y. H. Kuo, 1987: Description of the Penn State/NCAR Meso-scale Model Version 4 (MM4). NCAR Tech. Note, NCAR/TN-282+STR, 66 pp.

Ardanuy, P., 1979: On the observed diurnal observation of the Somali jet. *Mon. Wea. Rev.,* **107,** 1694–1700.

Baines, P. G., 1995: *Topographic Effects in Stratified Flows.* Press Syndicate of the University of Cambridge, 482 pp.

Bannon, P. R., 1979: On the dynamics of the East African Jet. I: Simulation of the mean conditions for July. *J. Atmos. Sci.,* **36,** 77–90.

Camberlin, P., and J. G. Wairoto, 1997: Intraseasonal wind anomalies related to wet and dry spells during the long and short rainy seasons in Kenya. *Theor. Appl. Climatol.,* **58,** 57–69.

Chen, Y., X. A. Chen, and Y. Zhang, 1994: A diagnostic study of the low-level jet during TAMEX IOP 5. *Mon. Wea. Rev.,* **122,** 2257–2284.

Cook, K. H., 1999: Generation of the African Easterly Jet and its role in determining West African precipitation. *J. Climate,* **12,** 1165–1184.

Cressman, G. P., 1979: An operational objective analysis system. *Mon. Wea. Rev.,* **87,** 367–381.

Doswell, C. A., 1977: Obtaining meteorologically significant surface divergence fields through the filtering property of objective analysis. *Mon. Wea. Rev.,* **105,** 885–892.

Eliassen, A., 1949: The quasi-static equations of motion with pressure as independent variable. *Geofys. Publ.,* **17,** 44 pp.

Findlater, J., 1966: Cross-equatorial jet streams at low-levels over Kenya. *Meteor. Mag.,* **95,** 353–364.

——, 1977: Observational aspects of the low level cross-equatorial jet stream of the western Indian Ocean. *Pure Appl. Geophys.,* **115,** 1251–1262.

Giorgi, F., and M. R. Marinucci, 1991: Validation of a regional atmospheric model over Europe: Sensitivity of wintertime and summertime simulations to selected physics parameterizations and lower boundary conditions. *Quart. J. Roy. Meteor. Soc.,* **117,** 1171–1206.

——, and L. O. Mearns, 1999: Regional climate model revisted. *J. Geophys. Res.,* **104,** 6335–6352.

——, M. R. Marinucci, and G. T. Bates, 1993a: Development of a second-generation regional climate model (RegCM2). Part I: Boundary-layer and radiative transfer processes. *Mon. Wea. Rev.,* **121,** 2794–2813.

——, ——, ——, 1993b: Development of a second-generation regional climate model (RegCM2). Part II: Convective processes and assimilation of lateral boundary conditions. *Mon. Wea. Rev.,* **121,** 2814–2832.

Grell, G. A., 1993: Prognostic evaluation of assumptions used by cumulus parameterizations. *Mon. Wea. Rev.,* **121,** 764–787.

Hastenrath, S., 1985: *Climate and Circulation of the Tropics.* D. Reidel Publishing Company, 455 pp.

Holtslag, A. A. M., E. I. F. de Bruijn, and H. L. Pan, 1990: A high-resolution air mass transformation model for short-range weather forecasting. *Mon. Wea. Rev.,* **118,** 1561–1575.

Hsie, E. Y., R. A. Anthes, and D. Keyser, 1984: Numerical simulation of frontogenesis in a moist atmosphere. *J. Atmos. Sci.,* **41,** 2581–2594.

Indeje, M., and E. K. Anyamba, 1998: Sensitivity of mesoscale systems over Kenya to changes in roughness length. *J. Afr. Meteor. Soc.,* **3,** 19–33.

——, F. H. M. Semazzi, and L. J. Ogallo, 2000: ENSO signals in East African rainfall seasons. *Int. J. Climatol.,* **20,** 19–46.

Ininda, J. M., 1998: Simulation of the impact of sea surface temperature anomalies on the short rains over East Africa. *J. Afr. Meteor. Soc.,* **3,** 127–138.

Kasahara, A., 1966: The dynamical influence of orography on the

large-scale motion of the atmosphere. *J. Atmos. Sci.,* **23,** 259–270.

Kida, H., T. Koide, H. Sasaki, and M. Chiba, 1991: A new approach for coupling a limited area model to a GCM for regional climate simulations. *J. Meteor. Soc. Japan,* **69,** 723–728.

Kiehl, J. T., J. J. Hack, G. B. Bonan, B. A. Boville, D. L. Williamson, and P. J. Rasch, 1998: The National Center for Atmospheric Research Community Climate Model: CCM3. *J. Climate,* **11,** 1131–1150.

Kinuthia, J. H., 1992: Horizontal and vertical structure of the Lake Turkana jet. *J. Appl. Meteor.,* **31,** 1248–1274.

——, and G. C. Asnani, 1982: A newly found jet in North Kenya (Turkana Channel). *Mon. Wea. Rev.,* **110,** 1722–1728.

Krishnamurti, T. N., 1961: The subtropical jetstream of winter. *J. Meteor.,* **18,** 172–191.

——, J. Molinari, and H. L. Pan, 1976: Numerical simulation of the Somali jet. *J. Atmos. Sci.,* **33,** 2350–2362.

——, R. J. Pasch, and P. Ardanuy, 1980: Prediction of African waves and specification of squall lines. *Tellus,* **32,** 215–231.

Lumb, F. E., 1966: Synoptic disturbances causing rainy periods along the East African coast. *Meteor. Mag.,* **95,** 150.

Mukabana, J. R., and R. A. Pielke, 1996: Investigating the influence of synoptic-scale monsoonal winds and mesoscale circulations and diurnal weather patterns over Kenya using a mesoscale numerical model. *Mon. Wea. Rev.,* **124,** 224–243.

Murakami, T., and W. L. Sumathipala, 1989: Westerly bursts during the 1982/83 ENSO. *J Climate,* **2,** 71–85.

Ngara, T., and G. C. Asnani, 1978: Five-day oscillation in the East African low-level jet. *Nature,* **272,** 708–709.

Nicholson, S. E., 1996: A review of Climate Dynamics and Climate Variability in Eastern Africa. *The Limnology, Climatology and Paleoclimatology of the East African Lakes,* Gordon and Breach, 57 pp.

Ogallo, L. J., 1980: Rainfall variability in Africa. *Mon. Wea. Rev.,* **107,** 1133–1139.

Okeyo, A. E., 1986: The influence of Lake Victoria on the convective systems over the Kenya highlands. *Proc. Int. Conf. on Short, Medium range Weather Forecasting.* Tokyo, Japan, WMO Rep., 40–47.

Okoola, R. E., 1999: A diagnostic study of the eastern Africa monsoon circulation during the Northern Hemisphere spring season. *Int. J. Climatol.,* **19,** 143–168.

Patwardhan, S. K., and G. C. Asnani, 1999: Meso-scale distribution of summer monsoon rainfall near the western Ghats (India). *Int. J. Climatol.,* **20,** 575–581.

Ramachandran, G., K. V. Rao, and K. Krishna, 1980: An observational study of the boundary layer winds in the exit region of a mountain gap. *J. Appl. Meteor.,* **19,** 881–888.

Ringler, T. D., and K. H. Cook, 1999: Understanding the seasonality of the orographically forced stationary waves: Interaction between mechanical and thermal forcing. *J. Atmos. Sci.,* **56,** 1154–1174.

Sarker, R. P., K. C. Sinha, and U. S. De, 1978: Dynamics of orographic rainfall. *Indian J. Meteor. Hydrol. Geophys.,* **29,** 335–348.

Semazzi, H. F. M., 1980: Stationary barotropic flow induced by a mountain over a tropical belt. *Mon. Wea. Rev.,* **108,** 922–930.

——, 1985: An investigation of the equatorial orographic dynamic mechanism. *J. Atmos. Sci.,* **42,** 28–83.

——, and L. Sun, 1997: The role of orography in determining the Sahelian climate. *Int. J. Climatol.,* **17,** 581–596.

Shea, D. J., K. E. Trenberth, and R. W. Reynolds, 1992: A global monthly sea surface temperature climatology. *J. Climate,* **5,** 987–1001.

Stull, B. S., 1988: *An Introduction to Boundary Layer Meteorology.* Kluwer Academic Publishers, 666 pp.

Sun, L., F. H. M. Semazzi, F. Giorgi, and L. J. Ogallo, 1999a: Application of the NCAR Regional Climate Model to Eastern Africa. Part I: Simulations of Autumn Rains of 1988. *J. Geophys. Res.,* **104,** 6529–6548.

——, ——, ——, ——, 1999b: Application of the NCAR Regional Climate Model to Eastern Africa. Part II: Simulations of Interannual Variability. *J. Geophys. Res.,* **104,** 6549–6562.

Thompson, P. D., 1957: A heuristic theory of large-scale turbulence and long period velocity variations in barotropic flow. *Tellus,* **9,** 69–91.

Wiin-Nielsen, A., 1961: On short and long term variations in quasi-barotropic flow. *Mon. Wea. Rev.,* **89,** 461–476.

Xue, M., and A. J. Thorpe, 1991: A mesoscale numerical model using the nonhydrostatic pressure-based sigma-coordinate equations: Model experiments with dry mountain flow. *Mon. Wea. Rev.,* **119,** 1168–1185.

Xue, Y., and J. Shukla, 1998: Model simulation of the influence of Global SST anomalies on Sahel rainfall. *Mon. Wea. Rev.,* **126,** 2782–2792.